Surface Science 605 (2011) 390–395

Contents lists available at ScienceDirect

Surface Science

journal homepage: www.elsevier.com/ locate/susc

Coherent scattering from silicon monocrystal surface

F. Livet [a,*], G. Beutier [a,e], M. de Boissieu [a], S. Ravy [b], F. Picca [b], D. Le Bolloc'h [c], V. Jacques [d,c]

[a] SIMaP, Grenoble-INP, CNRS, UJF, BP 75, 38402 Saint Martin D'Hères, France
[b] Synchrotron Soleil, L'Orme des Merisiers, Saint-Aubin, BP 48, 91192 GIF-sur-YVETTE, France
[c] LPS, CNRS, Université Paris Sud, Bâtiment 510, 91405 Orsay, France
[d] ESRF, BP 220, 38043 Grenoble, Cedex 9, France
[e] Diamond Light Source, Didcot, Oxfordshire OX11 0DE, UK

ARTICLE INFO

Article history:
Received 27 April 2010
Accepted 9 November 2010
Available online 23 November 2010

Keywords:
Coherent X-rays
Surface X-ray scattering
Anti-Bragg
Speckles
Atomic steps

ABSTRACT

Using coherent X-ray scattering, we evidenced atomic step roughness at the (111) vicinal surface of a silicon monocrystal of 0.05° miscut. Close to the $\frac{1}{2}\frac{1}{2}\frac{1}{2}$ anti-Bragg position of the reciprocal space which is particularly sensitive to the (111) surface, the truncation rod exhibits a contrasted speckle pattern that merges into a single peak closer to the 111 Bragg peak of the bulk. The elongated shape of the speckles along the (111) direction confirms the monoatomic step sensitivity of the technique. This experiment opens the way towards studies of step dynamics on crystalline surfaces.

© 2010 Elsevier B.V. All rights reserved.

1. Introduction

The surface of crystals is extensively studied because it is the region of the sample where elements are aggregated from liquid, vapor or solid phases. Numerous microscopies have been developed for the observation of surface topography. Optical or Scanning Electron Microscopy methods are the simplest [1]. Low energy electron microscopy [2,3] and near field methods (AFM, MFM, and STM) [4,5], are now classical methods for the study of the static surface configuration.

An important subject of the surface study is the direct observation of the dynamics of the surface fluctuations connected to surface step movement [6–8], to change in crystal shape by nucleation and/or annihilation of steps at face edges [9] or to the fluctuations of chemically inhomogeneous surfaces [10]. The main available experimental method for the observation of surface dynamics is time-resolved STM, where the movement of an individual step is observed by successive linear scans across a reduce segment. In these experiments, the evolution of the step position is recorded, and from a series of measurements, a statistical study provides information on the dynamics of surface evolution [8,11]. This method provides measurements of the step dynamics for times ranging between 0.1 and a few tens of seconds and for distances between 0.1 and a few tens of nanometers. These very local measurements provide accurate knowledge of the atomic surface properties, and the various atomic models of the dynamics can be discussed [12].

X-ray diffraction has also been proved a very useful method for surface observation [13]. The regions of the reciprocal space where valuable information about the surface morphology can be obtained are the "crystal truncation rods" (CTR). CTR are satellite streaks perpendicular to the surface originating from Bragg peaks, and by analogy, specular reflectivity can be considered as the satellite of the (000) reciprocal position. The longitudinal variations of CTR intensity have been extensively used for the observation of the change in atomic position [14] and in atomic composition in the vicinity of the surface [15,16] and of surface roughness [17].

Moreover, the transverse intensity of the CTR corresponds to the Fourier transform of the surface topography. Qualitatively, the relative distance ($\Delta Q \simeq 2\pi/e$) of the reciprocal point of the CTR from the nearest Bragg peak samples a thickness e under the surface. The special position intermediate between two Bragg peaks essentially corresponds to surface defects of monoatomic thickness (steps, monoatomic layers…) and is called the "anti-Bragg" (AB) region. At this point, perfectly flat diffracting planes scatter with relative phase shifts of π, cancelling each other and only the scattering of the cut-off introduced by the surface is observed.

In this region, the cross section is very low, and the Bragg to AB cross section ratio roughly corresponds to the square of the ratio between the number of volume atoms and the number of surface atoms in the coherence volume [13]. The AB intensity is also proportional to the number of irradiated surface atoms, and measurements are often carried out in asymmetric geometry, with a low incident angle.

* Corresponding author.
E-mail address: frederic.livet@simap.grenoble-inp.fr (F. Livet).

0039-6028/$ – see front matter © 2010 Elsevier B.V. All rights reserved.
doi:10.1016/j.susc.2010.11.006

In this paper, we show that the CTR transverse intensity in the conditions of coherent diffraction can provide a new method for the observation of steps at the surface of crystals and that this method can be extended to dynamical surface studies.

2. Description of the experiment

Fig. 1 gives a rapid scheme of the setup used for this type of experiment. Coherent diffraction from a sample can be observed if the irradiated volume has the size of the coherence volume [18]. A good transverse coherence length is obtained by using suitable slits, in order that the product of the beam size at sample ϕ by the beam divergence ε is of the order of the wavelength λ [19]. The longitudinal coherence length Λ_l is fixed by the beam monochromaticity $\Lambda_l = \lambda^2/2\Delta\lambda$, typically 0.6 μm at 7 keV and the path-length difference $\Delta\mathcal{L}$ of the beam scattered in the sample must not exceed this limit. The scattering vector $\vec{Q}$ where measurements are carried out here is far enough from Bragg peaks, and only interferences between surface atoms are relevant. For a miscut angle α (see Fig. 1) between the surface normal and $\vec{Q}$, which we decompose in a component $\alpha_\parallel$ in the diffraction plane and $\alpha_\perp$ in the direction perpendicular to this plane, the path-length differences can be written:

$$\Delta\mathcal{L} \simeq 2\phi \times \alpha_\parallel \leq \Lambda_l \quad (1)$$

and:

$$\Delta\mathcal{L} \simeq 2\phi \tan(\alpha_\perp)\sin(\theta) \leq \Lambda_l. \quad (2)$$

From Eq. (1), one observes that the scattering geometry must be roughly symmetric ($\alpha_\parallel \leq 1-2°$) and that even for symmetric diffraction, from Eq. (2), one must fulfill: $\tan\alpha_\perp \leq \Lambda_l/(2\phi\sin(\theta))$ (i.e. $\alpha_\perp \leq 5°$ here).

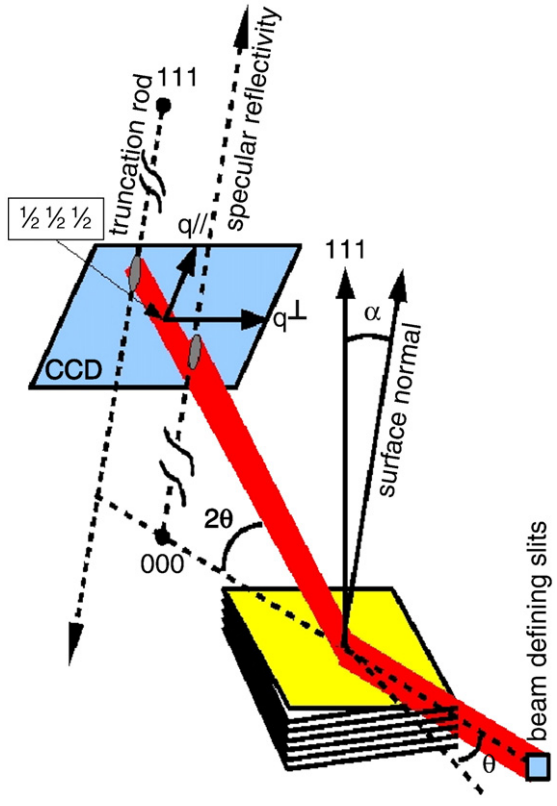

Fig. 1. Description of the experiment. The diffraction plane is vertical. The silicon crystal miscut angle is $\alpha \simeq 0.05°$. The CCD selects a small planar area of the reciprocal space and intercepts the (111) direction with an angle θ. With our small miscut, the CCD area intercepts both the specular reflection and the truncation rod from the (111) Bragg peak. The direction $q_\perp$ is horizontal and $q_\parallel$ is in the vertical diffracting plane.

In order to demonstrate the feasibility of our approach, we have chosen to test a silicon crystal with a very small misorientation of the [111] axis relative to the surface normal (a vicinal surface with an $\alpha \simeq 0.05°$ miscut). Silicon was chosen because of its perfect crystallinity, with no structure defects except surface. The perfect crystallinity is a key requirement of the method in order to ascribe the speckles to surface defects with confidence. Moreover, silicon has the advantage that it can be studied in air and at room temperature. The crystal studied here had been carefully polished by the ESRF staff for monochromator use. Laboratory X-ray reflectivity measurements showed a few Angstroms rugosity of the surface and a very thin (less than 1 nm on average) layer of silicon oxide. Coherent X-ray scattering experiments were performed at the CRISTAL beamline of the synchrotron SOLEIL. The 1.772 Å (7 keV) wavelength was selected with a Si_{111} double crystal monochromator and mirrors were used for harmonic suppression. Transverse coherence is achieved by combining two sets of square slits, one 13 m upward, with a 100 to 250 μm aperture and one close (0.15 m) to the sample, with 10 to 20 μm apertures. With this setup, we can adjust the balance between intensity and coherence. Speckles of reasonable contrast were observed with the larger apertures, the beam intensity being in the 5.10^8 ph/s range after the slits.

The sample was in air and positioned precisely at the center of the "kappa geometry" goniometer of the beamline. The scattering plane was vertical. Scattering was measured with a back illuminated CCD from Andor Technologies (1024 × 1024 pixels of 13 μm size) located at 2.2 m. The pixel resolution of this setup is $\delta q \simeq 2.1 \times 10^{-5}$ Å^{-1}. A dedicated program was used for individual photon extraction from electronic noise [20,21]. This is critical for such low intensity measurements. Indeed, the intensity at the AB position is eight orders of magnitude weaker than the incident beam. It also restores the pixel resolution of the CCD. Static images were obtained from the accumulation of at least 100 frames. With the fast (2.5 MHz) converter, good quality images could be obtained in one minute for large enough intensity. For all figures of this paper, a 2 × 2 merge of the CCD pixels has been performed. This improves statistics, and it does not significantly alter the speckle contrast.

3. Typical results

Diffraction was studied in the vicinity of the *hhh* positions, *h* varying from 1/2 to 1. In Fig. 1, the reciprocal lattice plane observed for $h = 1/2$ (AB position between the 000 and 111 reciprocal lattice points) is schematized. This plane intercepts the specular and the truncation rods close to the exact AB position, due to the small misfit. Fig. 2 shows a typical image of the diffracted intensity around the AB position.

Although the area of the reciprocal space covered by our detector is very small, we observe here two peaks, with $n_\parallel = 550$ pixels and $n_\perp = 50$ pixels spacings in the $q_\perp$ and $q_\parallel$ directions respectively. The higher intensity peak (about 2 ph/s integrated intensity) corresponds to the truncation rod originating from the 111 Bragg reflection and the lower intensity one (about 0.3 ph/s integrated intensity) to the surface reflectivity. Both peaks are roughly aligned in the vertical direction of the detector, essentially because the CTR is intercepted with a small θ angle (8°). Upon azimuthal rotation of the sample around its surface normal, they rotate around each other along an ellipse elongated by a factor $1/\sin(\theta)$ along $q_\parallel$. The distance between these two peaks provides a very precise estimate of the miscut α. In the configuration of Fig. 2, we obtain: $\alpha_\parallel = n_\parallel 13.10^{-6}/(4 \times 2.2) = 0.047°$ and $\alpha_\perp = n_\perp 13.10^{-6}/(4 \times 2.2 \sin(\theta)) = 0.030°$ which gives the miscut angle: $\alpha = \sqrt{\alpha_\parallel^2 + \alpha_\perp^2} = 0.056°$.

The lower intensity peak, detailed in Fig. 3(a), is a large $\left|\vec{Q}\right|$ measurement of the specular reflectivity and its intensity is connected

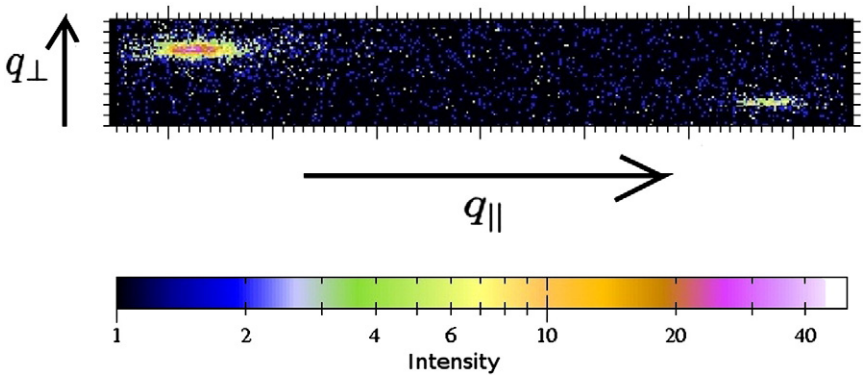

Fig. 2. Scattering intensity in the vicinity of the $(\frac{1}{2}\frac{1}{2}\frac{1}{2})$ AB position. Only a small region of interest of 700×100 pixels ($\Delta q_{||} \simeq 1.46\times10^{-2}$ Å^{-1} and $\Delta q_\perp \simeq 2.1\times10^{-3}$ Å^{-1}) of the CCD was used for this figure. Log units, maximum intensity for the CTR is 50 ph/pixel for a 2500 s acquisition time. Air scattering is less than one count.

to surface rugosity. This intensity corresponds to an electromagnetic amplitude scattered from the silicon crystal surface rugosity and its thin amorphous silicon oxide layer. In our laboratory experiment (incoherent scattering) we have observed that the contribution of this oxide layer lowers the pure silicon reflectivity by roughly an order of magnitude in this Q range.

The synchrotron experiment described here differs from incoherent scattering experiments: in a laboratory experiment, the irradiated region of the sample ranges in millimeters with less than 1 μm transverse coherence length, while here, all the illuminated 140 μm×20 μm region scatters coherently.[1] This leads to the formation of contrasted speckles in both peaks, as seen in Fig. 3 (linear plot), where we detail the shape of the two peaks.

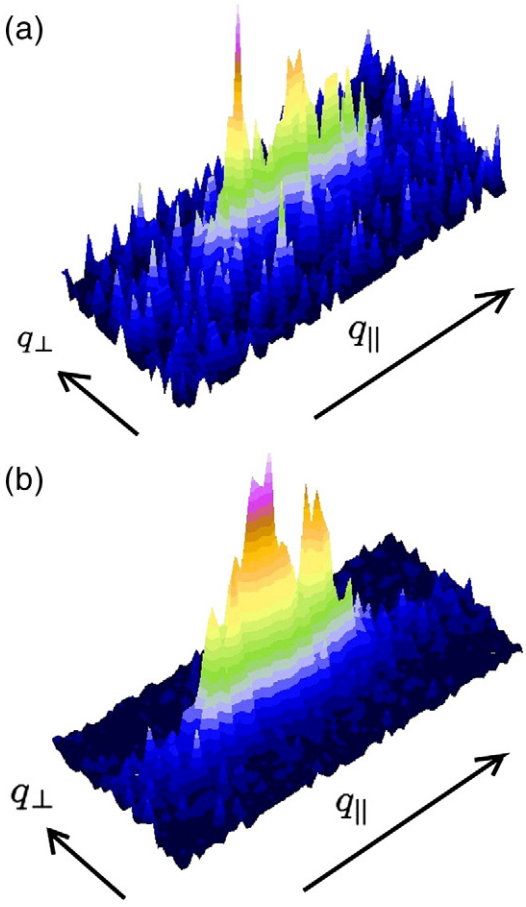

Fig. 3. Details of the transverse shape of the specular peak (a) and of the 111 truncation rod (b) of Fig. 2. In both figures, a 120×56 pixel region was selected ($\Delta q_{||} \simeq 2.52\times10^{-3}$ Å^{-1} and $\Delta q_\perp \simeq 1.18\times10^{-3}$ Å^{-1}). The maximum intensity is 15 counts in (a) and 50 in (b). Air scattering is less than one count.

In this figure, we observe that both peaks are elongated in the $q_{||}$ direction. We clearly observe in Fig. 3(b) a speckle structure. The same can be observed in Fig. 3(a), despite the low intensity. This speckle structure is connected to the local configuration of the surface and corresponds to the interferences occurring between the electromagnetic waves scattered by various regions of the surface. This typical behavior was observed for much smaller θ angles by Robinson et al. [22], with a much larger elongation.

The CTR peak has a well identified speckle pattern, as shown in Fig. 4. This figure is the result of the scan along the CTR, h varying from 0.5 to 0.81. This speckle structure is connected to the morphology of the Si [111] crystalline surface. It is only sensitive to the crystalline character of the sample surface, and the amorphous surface oxide layer does not contribute to the amplitude observed. Between $h=0.5$ (Fig. 4a) and $h=0.56$ (Fig. 4b), the coherently irradiated region is roughly the same, and we observe that the transverse shape of the truncation rod has only small changes. The θ angle only varies from 8° to 9° ($\delta q = 0.12$ Å^{-1} along the (111) direction) and this is a 140 μm×20 μm irradiated area. As the speckle structure has slow variations along the (111) direction, the 3D intensity pattern in this coherent experiment is widely elongated in this direction. This indicates that the defects responsible for this pattern are surface defects, of atomic scale extension along the direction perpendicular to the surface.[2] This speckle structure is connected to the surface step configuration and it changes with the sample position. The average space between steps corresponding to the 0.056° miscut is 0.32 μm, for steps of the height of a silicon tetrahedron (0.314 nm). The intensity measured in the plane perpendicular to the CTR corresponds to the configuration of the surface monoatomic steps. For a well defined periodic step lattice, only a single peak is observed. In our case, speckles correspond to some disorder among these few hundred steps.

For values of (*hhh*) closer to (111) (Fig. 4d–f), the pattern is reduced essentially to a single peak. In this case, the small value of the difference $|\Delta\vec{Q}|$ between the Bragg peak and (*hhh*) makes the observation of the atomic scale surface defects difficult. The scattering corresponds to perfect atomic planes in the sample. In this case, diffraction does not significantly change the shape of the wave front of the incoming beam. This is shown in Fig. 5, where the cross-shaped diffracted beam reflects the slits selecting the coherent beam. Only for

[1] In this case, the maximum opening of the slits was used, this gives a 2.10^8 ph/s intensity, with a lower coherence contrast.

[2] Here, as we limit our study to $h<1$, the (111) atomic layers of silicon can be assumed as flat layers with a distance of $a/\sqrt{(3)} = 0.3136$ nm.

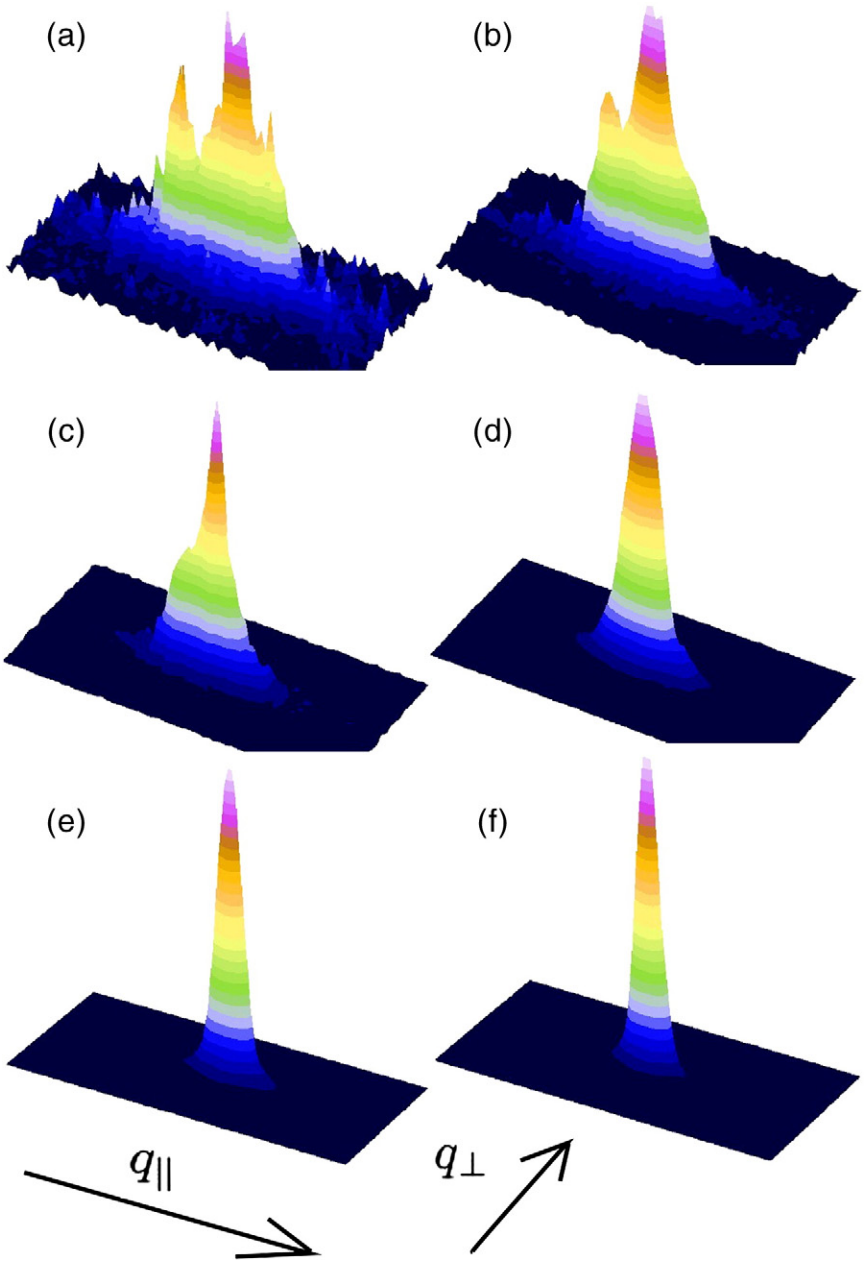

Fig. 4. The transverse shape of the truncation rod for various (h,h,h) vectors: (a) $h=0.5$, (b) $h=0.56$, (c) $h=0.63$, (d) $h=0.69$, (e) $h=0.75$, and (f) $h=0.81$. Intensities are in arbitrary linear units. Figures show the same number of detector pixels as in Fig. 3, i.e. total widths: $\Delta q_{\parallel} \simeq 2.52$ Å^{-3} and $\Delta q_{\perp} \simeq 1.18$ Å^{-3}. The distance $\delta h = 0.06$ corresponds to $\delta q = 0.12$ Å^{-1} along the (111) direction.

q value close to the Bragg peak (Fig. 5(c)) are observed typical fringes corresponding to slit scattering.

In Fig. 5, a diffuse streak is also observed, with a nearly 30° angle with the horizontal axis $q_{\perp}$, which we ascribe to residual strain of the crystal surface connected to polishing [23,24].

4. Discussion

We have shown that surface defects of monoatomic thickness can be observed from coherent scattering in the vicinity of the AB position. This is unambiguously observed because the underlying silicon crystal is free of dislocations or subgrain boundaries, as it can be verified from Fig. 5, where the CTR width is of the order of the experimental resolution. A complete calculation of surface scattering in these conditions and the detailed shape of the scattering in the very vicinity of the Bragg peak are out of the scope of this paper.

In this experiment, the intensity is low. Silicon is a rather light atom ($Z=14$), but the main reason is in the small number of atoms contributing to the measured interferences. The beam footprint is $\simeq 100\times 20\ \mu m^2$, and it is about 4×10^{10} atoms at the surface. The scale studied is intermediate between a classical incoherent experiment (a few mm^2) and a typical STM scan ($\simeq 0.1\ \mu m$). With appropriate optics and next generation sources (NSLS II, Petra III or even free-electron lasers), the beam intensity can be significantly improved, and on focusing, the beam footprint can be reduced to a few μm^2 area, with the same beam intensity.

The sample studied here has a perfect crystalline structure. In metallic crystals, defects like subgrain boundaries (mosaicity) make the observation of CTR speckles difficult. This means that experiments carried out on metal surfaces have to be combined with “in situ” annealing, in order to have subgrains of size larger than the beam. This is also easier to achieve with microbeams, and progress in focusing

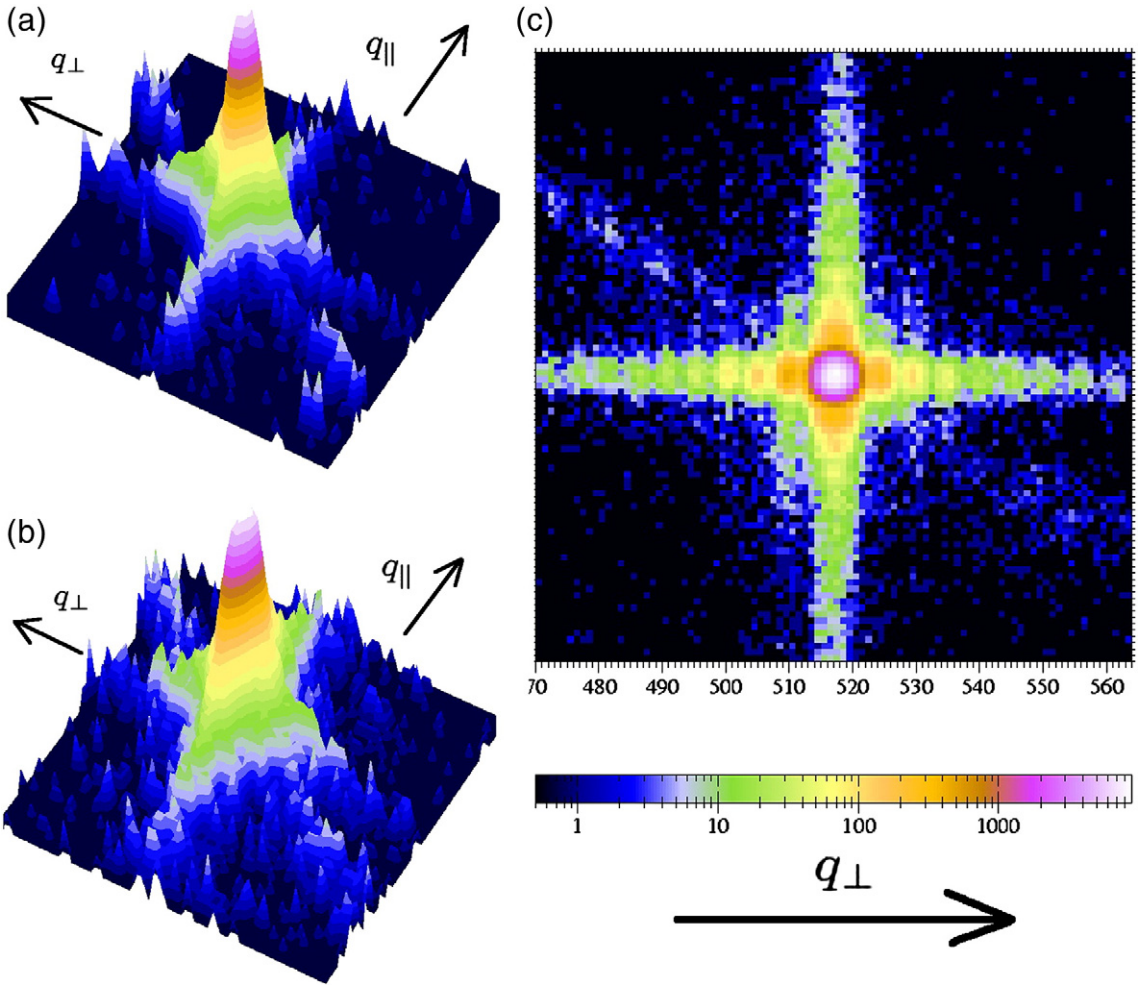

Fig. 5. The shape of the truncation rod in the vicinity of the Bragg peak (log units): (a) $h=0.94$ and (b) $h=0.875$ in the (hhh) direction. The cross corresponds to the diffraction of the slits limiting the beam ($\phi=20$ μm here). In (c) is shown the scattering with the aperture $\phi=10$ μm at $h=0.99$.

optics (refracting lenses, Fresnel lenses or "Kirkpatrick–Baez" mirrors) open the possibility of the "in situ" study of metal surfaces.

Roughly speaking, in the ideal case of "flat" surfaces with terraces separated by atomic steps, the number of speckles which share the rod intensity is of the order of the number of terraces in the beam. On reducing the size of the beam footprint, the number of speckles which share the diffracted intensity is reduced, and this eases their observation and the study of their dynamics.

In the case of metal surfaces, the observation of a small and adjustable area provides dynamical results over a set of defects, and X-ray Photon Correlation Spectroscopy [19,25] can be used for the study of step dynamics or of other surface defects, with a direct statistical analysis. This discussion can also be found in Ref. [26], where XPCS results of a study of the (100) surface of an Au single crystal are reported. With available synchrotrons, the accessible time scales range in minutes. With future X-ray sources, like the 4th generation free electron lasers, the peak brilliance should be increased of a factor 10^9 and the average brilliance of 10^4, opening access to millisecond time scale.

We have presented here a new and promising method for the study of surface dynamics. As focused beams open the possibility of varying the coherently irradiated area, the number of studied defects of the surface can be optimized, in order to obtain a statistical information. This will complete the STM studies where a single step is followed [8] and using X-rays will make possible measurements on buried interfaces, like between crystal and liquid or between two crystalline phases.

Acknowledgments

The authors are grateful to Benoît Picut from the ESRF optics laboratory for providing a high quality mechano-chemically polished silicon crystal.

The "fit2d" program from ESRF has been used for the figures.

Beamtime at the "Cristal" beamline was obtained under proposal no. 20080297, December 2008.

References

[1] D. Chatain, J. Métois, Surf. Sci. 291 (1993) 1.
[2] P. Müller, J.J. Métois, Surf. Sci. 599 (2005) 187.
[3] E. Bauer, Rep. Prog. Phys. 57 (1994) 895.
[4] S. Surnev, P. Coenen, B. Voigtländer, H.P. Bonzel, P. Wynblatt, Phys. Rev. 56 (1997) 12131.
[5] C. Barth, C.R. Henry, Phys. Rev. Lett. 98 (2007) 136804.
[6] L. Kuipers, M.S. Hoogeman, J.W.M. Frenken, H. van Beijeren, Phys. Rev. B 52 (1995) 11387.
[7] M. Giesen, G.S. Icking-Konert, Surf. Sci. 412/413 (1998) 645.
[8] D. Dougherty, O. Bondarchuk, M. Degawa, E. Williams, Surf. Sci. Lett. 527 (2003) L213.
[9] K. Thürmer, J.E. Reutt-Robey, E.D. Williams, M. Uwaha, A. Emundts, H.P. Bonzel, Phys. Rev. Lett. 87 (2001) 186102.
[10] I. Lyubinetsky, D.B. Dougherty, T.L. Einstein, E.D. Williams, Phys. Rev. B 66 (2002) 085327.
[11] E.L. Goff, L. Barbier, B. Salanon, Surf. Sci. 531 (2003) 337.
[12] M. Giesen, Prog. Surf. Sci. 68 (2001) 1.
[13] I.K. Robinson, Phys. Rev. B 33 (1986) 3830.
[14] I.K. Robinson, D.J. Tweet, Rev. Prog. Phys. 55 (1992) 599.
[15] I.K. Robinson, R.T. Tung, R. Feidenhans'l, Phys. Rev. B 38 (1988) 3632.

[16] O. Robach, H. Isern, P. Steadman, K.F. Peters, C. Quiros, S. Ferrer, Phys. Rev. B 68 (2003) 214416.
[17] A. Munkholm, S. Brennan, E.C. Carr, J. Appl. Phys. 82 (6) (1997) 2944. http://dx.doi.org/10.1063/1.366129, doi:10.1063/1.366129.
[18] M. Sutton, S.G.J. Mochrie, T. Greytak, S.E. Nagler, L.E. Berman, G.E. Held, G.B. Stephenson, Nature 352 (1991) 608.
[19] F. Livet, Acta Cryst. A-63 (2007) 87.
[20] F. Livet, F. Bley, J. Mainville, M. Sutton, S. Mochrie, E. Geissler, G. Dolino, D. Abernathy, G. Grübel, Nucl. Instr. Meth. A 451 (2000) 596.
[21] G. Beutier, G. van der Laan, A. Marty, F. Livet, Eur. Phys. J. Appl. Phys. 42 (2008) 161.
[22] I.K. Robinson, J.A. Pitney, J. Libbert, I. Vartanyants, Phys. B 248 (1998) 385.
[23] B. Croset, Y. Girard, G. PrÃ©vot, M.S.Y. Garreau, R. Pinchaux, M. Sauvage-Simkin, Phys. Rev. Lett. 88 (2002) 056103.
[24] G. Prévot, A. Coati, B. Croset, Y. Garreau, J. Appl. Cryst. 40 (2007) 874.
[25] G. Grübel, D.L. Abernathy, D.O. Riese, W.L. Vos, G.H. Wegdam, J. Appl. Cryst. 33 (2000) 424.
[26] M.S. Pierce, K.C. Chang, D. Hennessy, V. Komanicky, M. Sprung, A. Sandy, H. You, Phys. Rev. Lett. 103 (2009) 165501.